# Synthesis and characterization of Cu-Ni mixed metal paddlewheels occurring in the metal-organic framework DUT-8($Ni_{0.98}Cu_{0.02}$) for monitoring open-closed-pore phase transitions by X-band continuous wave EPR spectroscopy

## Supporting Information

Matthias Mendt[a,*], Sebastian Ehrling[b], Irena Senkovska[b], Stefan Kaskel[b], Andreas Pöppl[a]

[a]Felix Bloch Institute for Solid State Physics, Leipzig University, Linnéstr. 5, 04103 Leipzig, Germany

[b]Department of Inorganic Chemistry, Dresden University of Technology, Bergstr. 66, 01062 Dresden, Germany

[*]Email of corresponding author: matthias.mendt@uni-leipzig.de

## MOF characterization

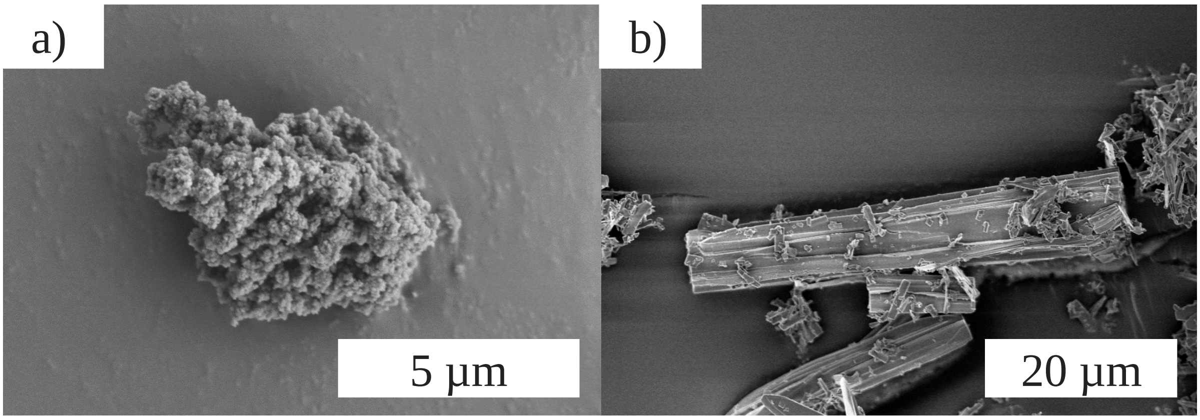


Figure S1. SEM pictures of the DUT-8($Ni_{0.98}Cu_{0.02}$) samples a) $\mathbf{1}_{act}$ and b) $\mathbf{2}_{act}$. Magnifications are displayed in the pictures.

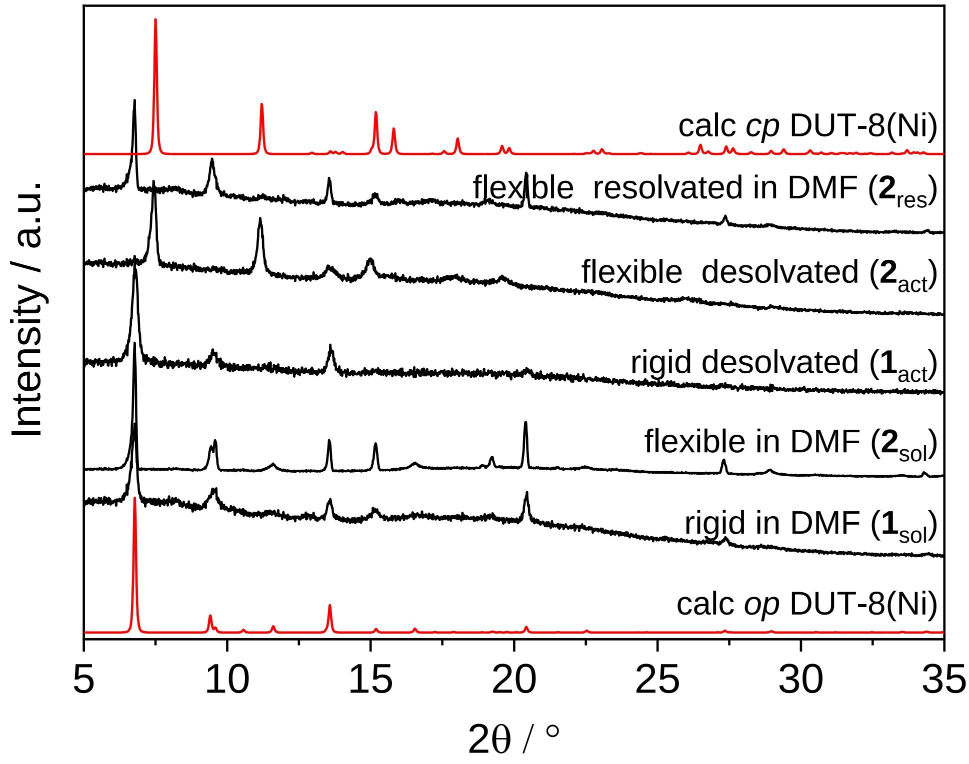


Figure S2. PXRD of DUT-8($Ni_{0.98}Cu_{0.02}$) samples in different conditions as marked in the figure. Here $\mathbf{1}_{sol}$ is the as made copper doped rigid DUT-8(Ni).

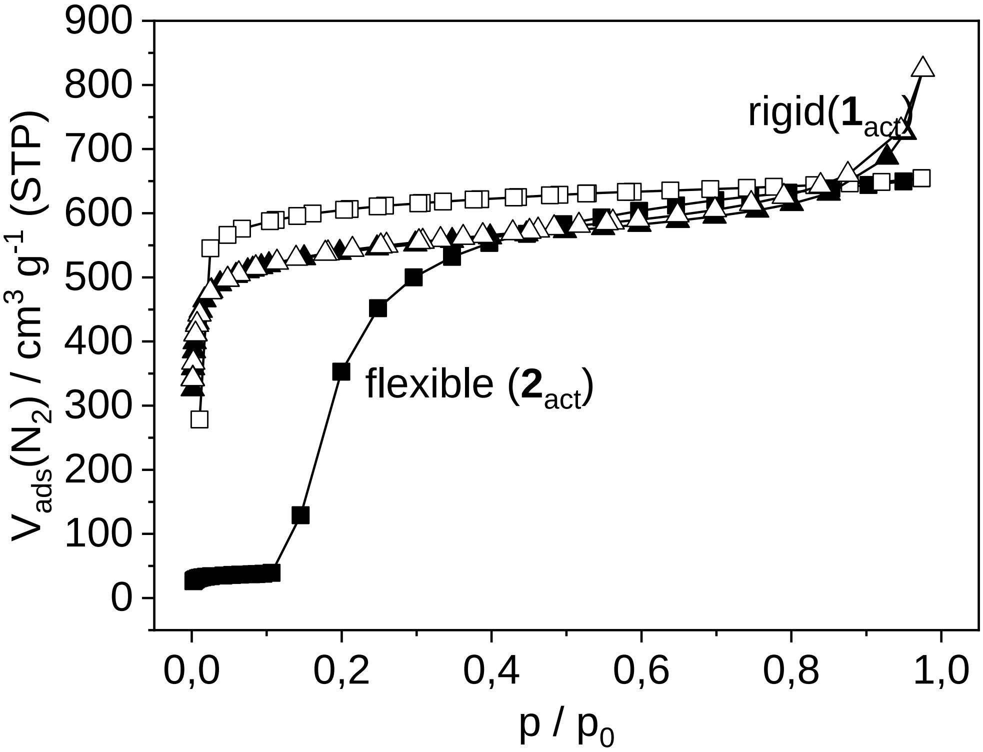


Figure S3. $N_2$ adsorption (filled symbols) and desorption (empty symbols) isotherms at $T$ = 77 K for $\mathbf{1_{act}}$ (triangles) and **2act** (squares).

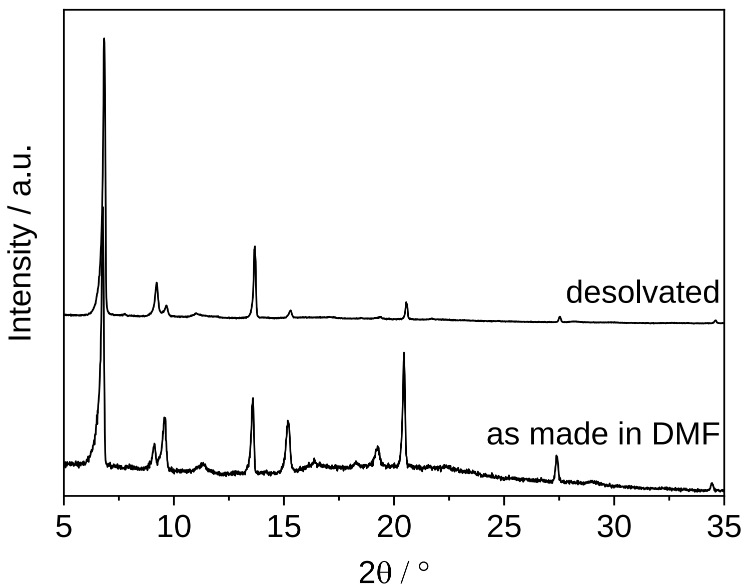


Figure S 4. PXRD of DUT-8(Cu) in its solvated form in DMF and its activated solvent free form

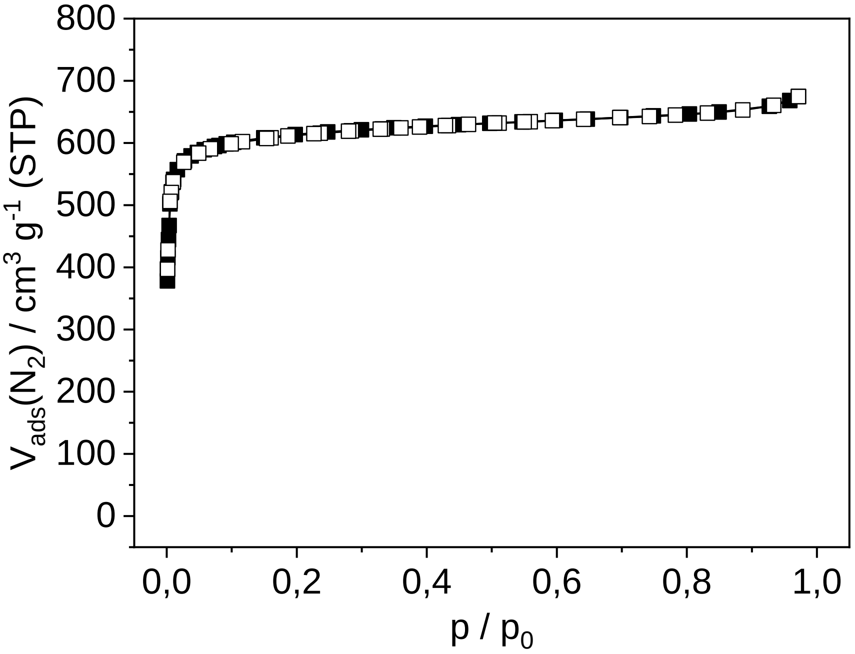


Figure S5. $N_2$ adsorption (filled squares) and desorption (empty squares) isotherms of DUT-8(Cu) at $T$ = 77 K.

## EPR Figures

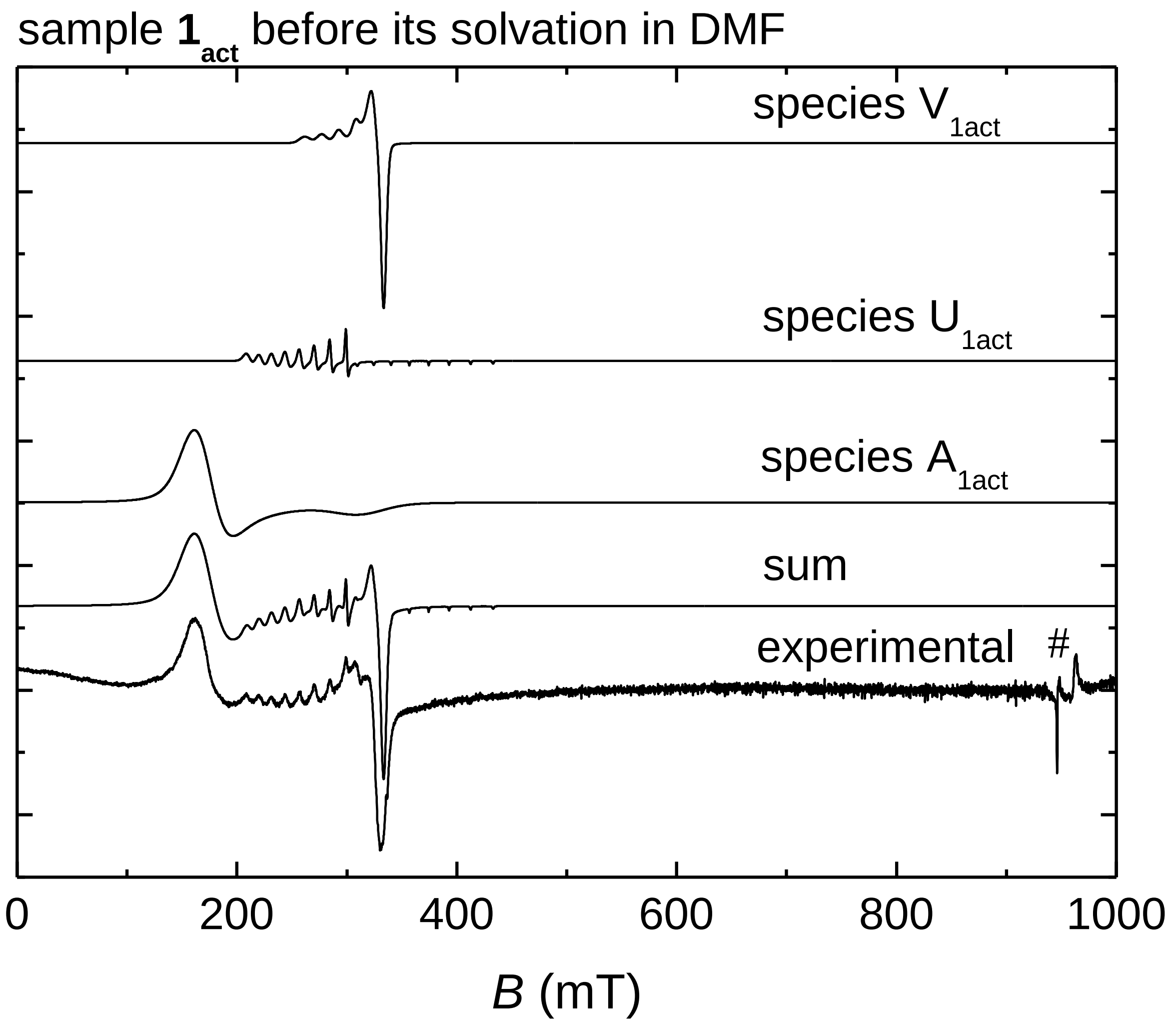


Figure S6. Experimental (bottom) and simulated EPR spectra of sample $\mathbf{1}_{act}$ before exactly the same sample was resolvated in DMF. The simulated signal (sum) is a superposition of the simulated signals of species $A_{1act}$, $U_{1act}$ and $V_{1act}$ as illustrated in the figure.

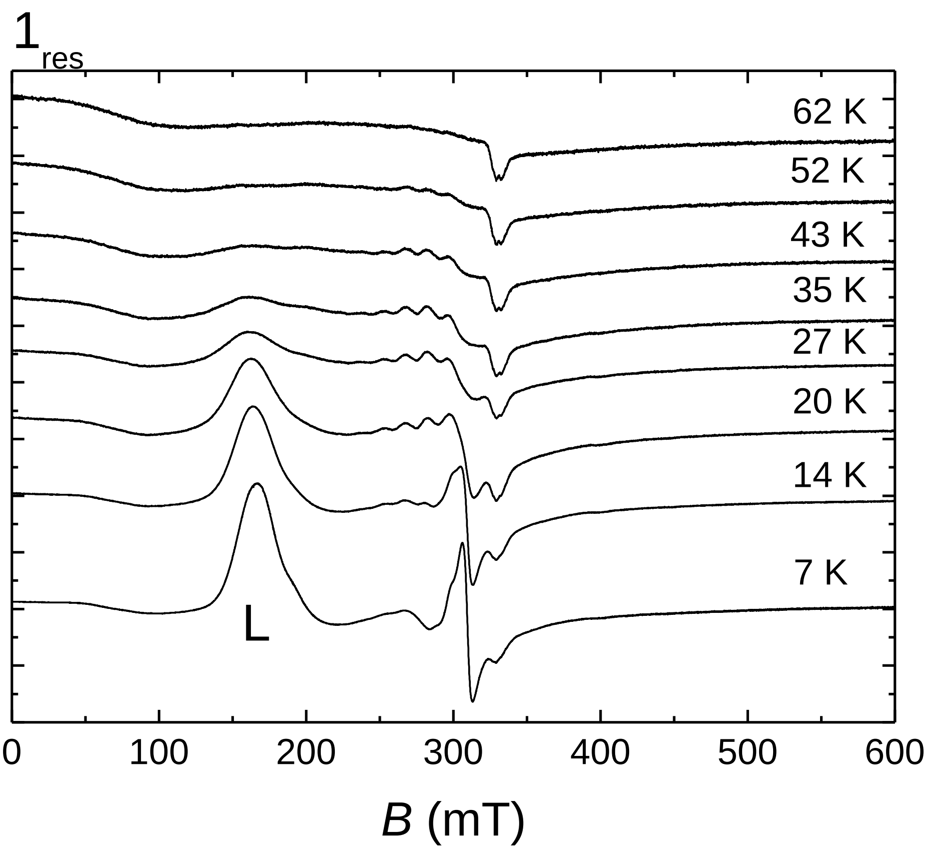


Figure S7. EPR spectra of sample $\mathbf{1_{res}}$ measured at different temperatures during heating.

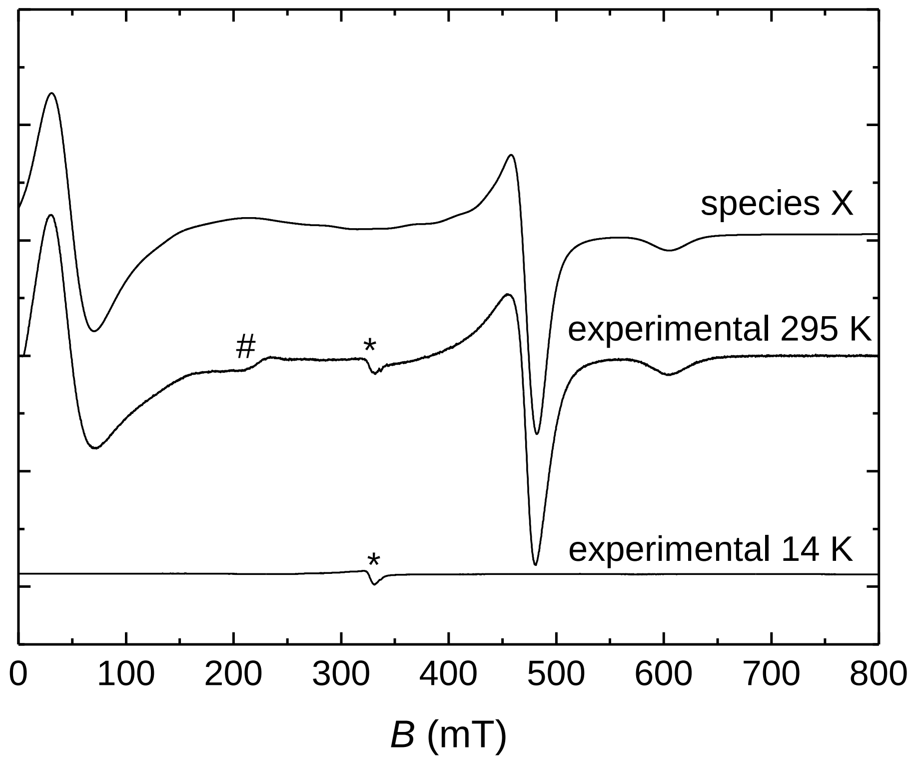


Figure S8. EPR spectra of the DUT-8(Cu) material as measured at $T$ = 295 K (middle) and $T$ = 14 K (bottom). The simulated signal of the $S$ = 1 species X is shown on top. The signal # is not assigned but might belong to that of species X and might not be revealed by the simulation due to inaccuracies in the line broadening model used for the spectral simulation of X. The signal * can be attributed to a monomeric $Cu^{2+}$ species ($S$ = 1/2) $M_0$ with g-tensor principle values $g_{xx,yy}$ = 2.05 ± 0.01 and $g_{zz}$ = 2.33 ± 0.01. The signal of $M_0$ at $T$ = 14 K further resolves the a $^{63}$Cu hyperfine interaction (hfi) splitting in z-direction of $A_{zz}^{^{63}\mathrm{Cu}} = 420 \pm 40$ MHz

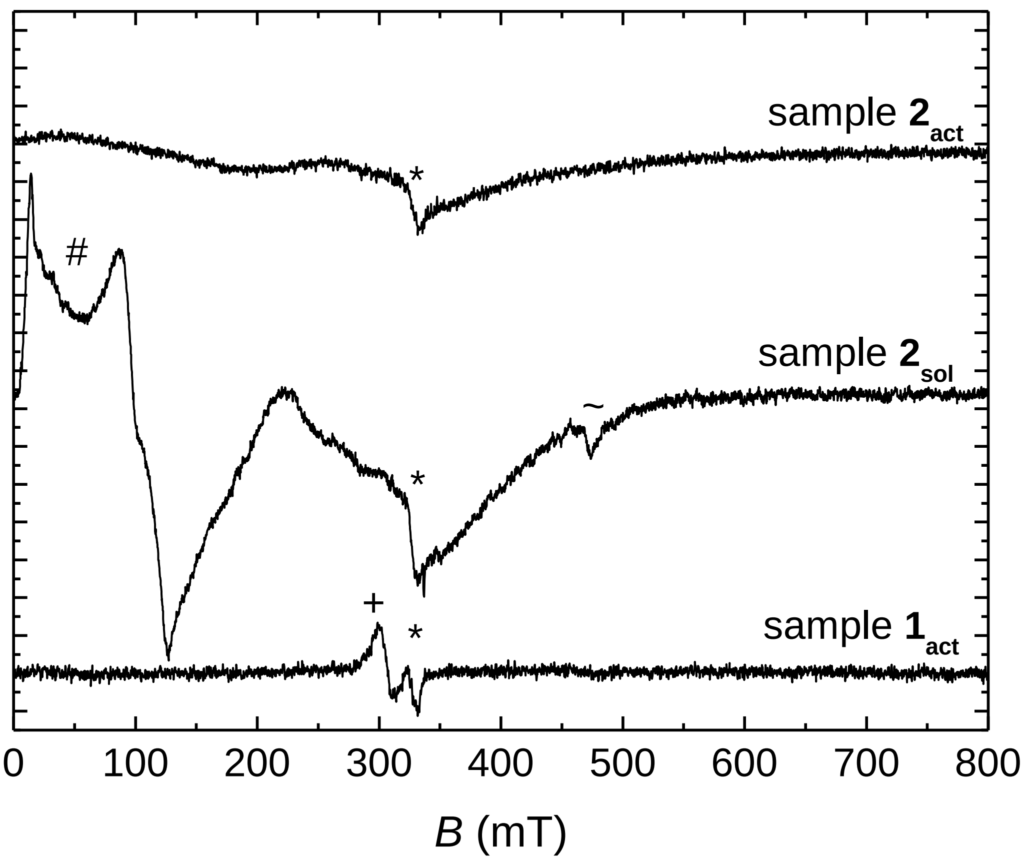


Figure S9. Experimental room temperature EPR spectra of sample $\mathbf{1}_{act}$ (rigid, desolvated), sample $\mathbf{2}_{sol}$ (flexible, solvated) and sample $\mathbf{2}_{act}$ (flexible, desolvated). The symbol * labels a $Cu^{2+}$ impurity of the cryostat or resonator. The signal + at $g$ = 2.19 might be attributed to monomeric $Ni^{+}$ or $Ni^{3+}$ impurities. The signal # in the field range 0 mT < $B$ < 220 mT might be assigned to a integer spin species called here $U_2$, like some $Ni^{2+}$ ($S$ = 1), dimeric $Ni^{2+}$-$Ni^{2+}$ ($S$ = 2) or dimeric $Cu^{2+}$-$Cu^{2+}$ ($S$ = 1) species. It is also present at $T$ = 14 K, but its signal intensity increases with increasing temperature (Figure 3c), indicating its likewise antiferromagnetic nature. We attribute the signal ~ to a minor fraction of monometallic Cu paddlewheel units, since it fits to the signal of species X.

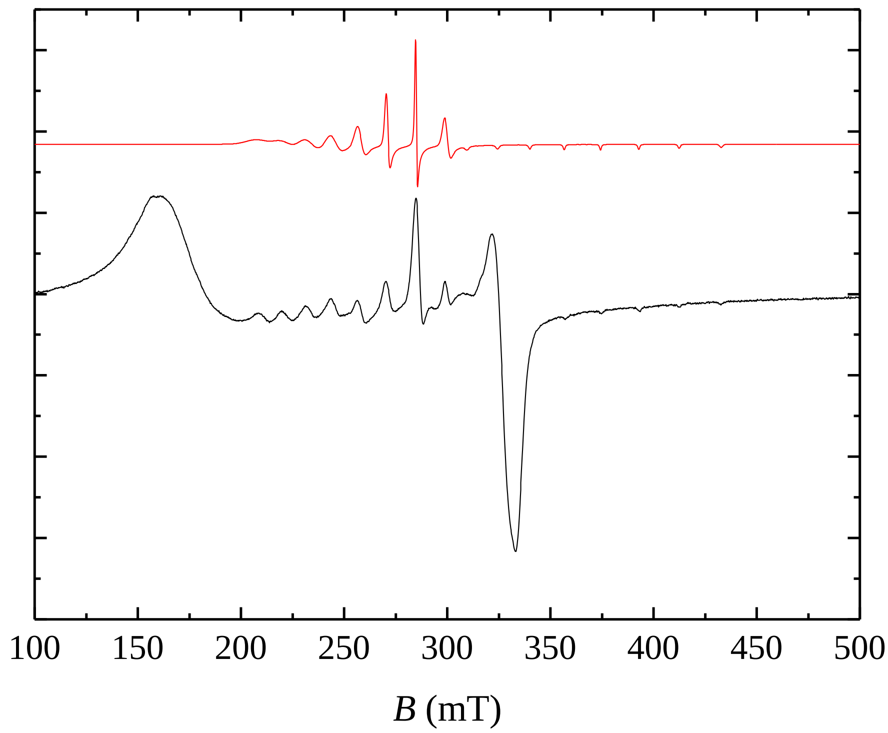


Figure S10. Experimental spectrum of sample $\mathbf{1}_{\mathbf{act}}$ at $T$ = 14 K (black) and the simulated signal of the $Co^{2+}$ containing species $U_1$ (red) assuming a positive g- and hfi correlation and a FWHM $\Delta A_{x,y} = 80$ MHz of the Gaussian distribution of the $A_{x,y}$ parameter.

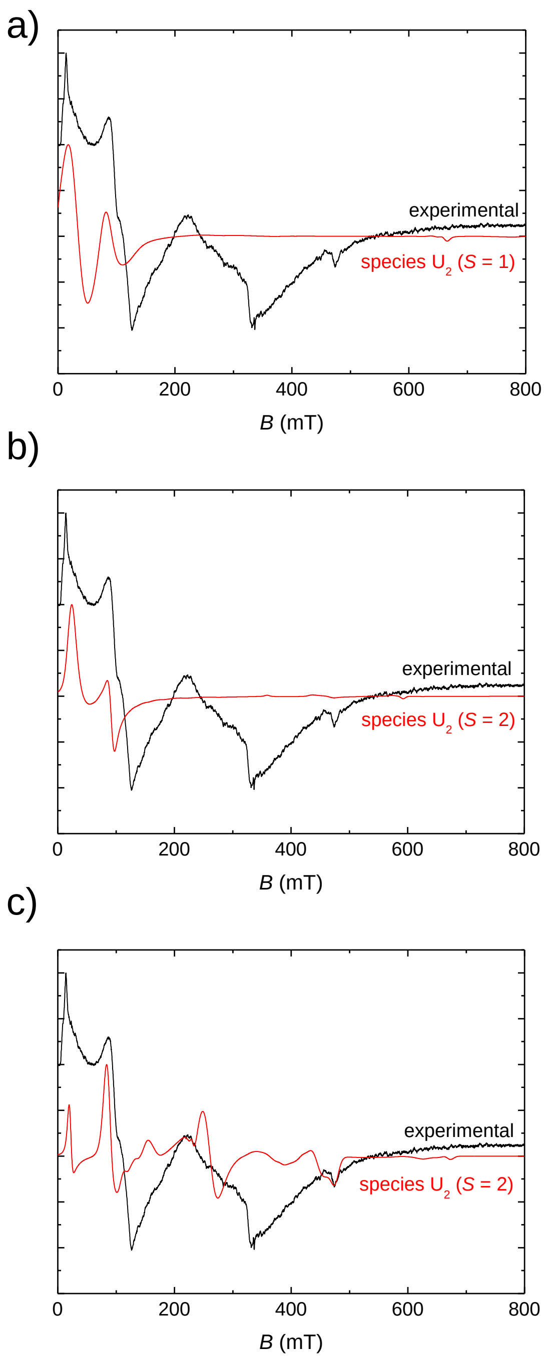


Figure S11. Experimental (black) and simulated (red) EPR spectra of sample $\mathbf{2}_{\mathbf{sol}}$ at room temperature illustrating the ambiguity interpreting species $U_2$. The simulations show three different possible examples how the EPR signal of species $U_2$ might be interpreted. In (a) an electron spin $S$ = 1 with g-tensor principle values $g_{xx,yy} \approx 2.5$, $g_{zz} \approx 2.0$ and fs parameters $D \approx$ 14700 MHz and $E/D \approx 0.32$ were assumed. For the simulation (b) an electron spin $S$ = 2, g-tensor principle values $g_{xx,yy} \approx 2.5$, $g_{zz} \approx 2.0$ and fs parameters $D \approx 21000$ MHz and $E/D \approx 0.25$ were assumed. For the simulation (c) an electron spin $S$ = 2, g-tensor principle values $g_{xx,yy} \approx 2.0$, $g_{zz} \approx 2.3$ and fs parameters $D \approx 4100$ MHz and $E/D \approx 0.12$ were assumed. Deviations between the experimental and simulated signal might be attributed to the restricted way simulating the g-strain and D-strain in EasySpin.[1]

# Tables

Table S 1. Linewidth parameters used for the simulations of the signals of different EPR active species, as they are defined by the MatLab toolbox EasySpin.[1] The values $\Delta g_x$, $\Delta g_y$, $\Delta g_z$, $\Delta D$ and $\Delta E$ are the full widths at half maximum (FWHM) of independent Gaussian distributions of the spin Hamiltonian parameters $g_x$, $g_y$, $g_z$, $D$ and $E$, respectively. The parameters $\delta B_{\mathrm{pp}}^{\mathrm{Gauss}}$ and $\delta B_{\mathrm{pp}}^{\mathrm{Lorentz}}$ are isotropic convolutional Gaussian and Lorentzian peak-to-peak linewidths.

| Species | $\Delta g_x$ | $\Delta g_y$ | $\Delta g_z$ | $\Delta D/D$ | $\Delta E/D$ | $\delta B_{\mathrm{pp}}^{\mathrm{Gauss}}$ (mT) | $\delta B_{\mathrm{pp}}^{\mathrm{Lorentz}}$ (mT) |
|---|---|---|---|---|---|---|---|
| X | - | - | - | 0.078 | 0.001 | 11.2 | 10.1 |
| $A_{1sol}$ | 0.3 | 0.3 | -[a] | - | - | 8 | 8 |
| $A_{1act}$ | 0.3 | 0.3 | -[a] | - | - | 10 | 10 |
| $A_{1res}$ | 0.3 | 0.3 | -[a] | - | - | 6 | 4 |
| $B_{1res}$ | 0.15 | 0.3 | -[a] | - | - | 2 | 2 |
| $A_{2sol,I}$ | 0.3 | 0.3 | 0.3 | - | - | 6 | 4 |
| $B_{2sol,I}$ | 0.15 | 0.15 | -[a] | - | - | 2 | 2 |
| $A_{2sol,II}$ | 0.3 | 0.15 | 0.3 | - | - | 6 | 4 |
| $B_{2act,I}$ | 0.3 | 0.3 | -[a] | - | - | 6 | 4 |
| $C_{2act,I}$ | - | - | - | 0.38 | 0.04 | 18 | 4 |
| $C_{2act,II}$ | 0.5 | 0.1 | -[a] | - | - | 18 | 4 |
| $D_{2act,III}$ | - | - | - | 0.4 | 0.04 | 22 | 8 |
| $E_{2act,III}$ | - | - | - | 0.4 | 0.04 | 22 | 26 |
| $A_{2res,I}$ | 0.3 | 0.3 | -[a] | - | - | 6 | 4 |
| $B_{2res,I}$ | 0.2 | 0.2 | -[a] | - | - | 2 | 2 |
| $A_{2res,II}$ | 0.15 | 0.3 | -[a] | - | - | 6 | 4 |

[a]not resolved

## Characterization of minor defect or impurity species

In this section minor EPR active species of defect or impurity nature are characterized and tentatively assigned without a detailed discussion.

Minor EPR signals measured for sample $\mathbf{1_{sol}}$ at $T$ = 14 K are illustrated in Figure 5a. The signal (+) at $g \approx 2.30$ might be assigned to some minor monomeric $Ni^{+}$ or low spin $Ni^{3+}$ defect or impurity species. The signal (*) at $g \approx 2.06$ might be assigned to some minor monomeric $Cu^{2+}$, $Ni^{+}$ or $Ni^{3+}$ species. An additional signal # at $g \approx 2.17$ might be tentatively assigned to some minor monomeric $Ni^{+}$ or low spin $Ni^{3+}$ defect or impurity species, both with electron spin $S$ = 1/2.

Minor EPR signals measured for sample $\mathbf{1_{res}}$ at $T$ = 7 K are illustrated in Figure 5c. The symbol ~ labels the signal attributed to the $Co^{2+}$ or $Ni^{2+}$-$Co^{2+}$ species $U_{1act}$ also observed for sample $\mathbf{1_{act}}$ (see below for spin Hamiltonian parameters). The signal (*) at $g \approx 2.06$ might be assigned to some minor monomeric $Cu^{2+}$, $Ni^{+}$ or $Ni^{3+}$ species. An additional signal # at $g \approx 2.17$ might be tentatively assigned to some minor monomeric $Ni^{+}$ or low spin $Ni^{3+}$ defect or impurity species, both with electron spin $S$ = 1/2. The signal + is attributed to a species $U_2$ that is described in more detail for sample $\mathbf{2_{sol}}$ (see below).

For sample $\mathbf{1_{act}}$ with the rigid activated MOF, we observed at $T$ = 14 K signals of two species $U_{1act}$ and $V_{1act}$ as shown in Figure 5b. We tentatively attribute species $U_{1act}$ to a minor monomeric $Co^{2+}$ low spin species ($S$ = 1/2) or to a minor dimeric $Ni^{2+}$-$Co^{2+}$ low spin species ($S$ = 1/2) with g-tensor principle values $g_{x,y} = 2.63 \pm 0.01$ and $g_z = 1.805 \pm 0.003$.[2] Its hyperfine interaction (hfi) to the $Co^{59}$ nucleus ($I$ = 7/2) shows a high resolution indicating a well-defined site of this species. The corresponding simulation derived principle values of the hfi tensor are $|A_{x,y}| = 470 \pm 15$ MHz and $|A_z| = 445 \pm 5$ MHz. The large intensity of the experimental $m_I = 5/2$ transition might be explained by correlated g- and hfi-strain effects as demonstrated by an exemplary simulation in the Figure S10. A satisfying agreement with the experimental linewidths and intensities of all hfi transitions was not achieved within the restricted linewidth model implemented in the MatLab toolbox EasySpin.[1] Minor contributions of $Co^{2+}$ impurities were also observed for the other samples, obeying similar spin Hamiltonian parameters. The cobalt impurities originate from the nickel source used for the synthesis of the materials. The question, if those $Co^{2+}$ ion are at $Ni^{2+}$ sites of the regular DUT-8 framework will be addressed in a future publication where cobalt doped DUT-8($Ni_{1-x}Co_x$) samples will be investigated by EPR.

Species $V_{1act}$ observed for sample $\mathbf{1}_{\mathbf{act}}$ at $T$ = 14 K (Figure 5b) can be tentatively assigned to a minor monomeric $Cu^{2+}$ species ($S$ = 1/2) or a low spin $Ni^{2+}$-$Cu^{2+}$ dimer with g-tensor principle values $g_{x,y} = 2.050 \pm 0.006$ and $g_z = 2.358 \pm 0.02$ and $Cu^{63}$ ($I$ = 3/2) hfi principle values $|A_{x,y}| < 80$ MHz and $|A_z| = 460 \pm 90$ MHz as they are typical for monomeric $Cu^{2+}$ in a square pyramidal coordination.[3,4] Since $Cu^{2+}$ sites in paddlewheel units of the DUT-8(Ni) **op** phase are expected to have an almost square pyramidal coordination[5] (Figure 1a), this species might be assigned to broken paddlewheel units where one $Ni^{2+}$ is substituted by $Cu^{2+}$ and the second $Ni^{2+}$ ion is missing.

For sample $\mathbf{2}_{\mathbf{sol}}$ containing the solvated flexible MOF a minor species $U_2$ with electron spin $S$ > 1/2 was observed at room temperature by its characteristic signal in the field range 0 mT < $B$ < 220 mT (Figure S9). It might be attributed to a species with an integer electron spin like a monomeric $Ni^{2+}$ impurity ($S$ = 1), a dimeric $Ni^{2+}$- $Ni^{2+}$ impurity ($S$ = 2) or a dimeric $Cu^{2+}$-$Cu^{2+}$ ($S$ = 1) species, as it is indicated by spectral simulations (ESI, Figure S11). It was neither observed for samples $\mathbf{1}_{\mathbf{act}}$ and $\mathbf{2}_{\mathbf{act}}$ (Figure S9) nor for the monometallic rigid and flexible DUT-8(Ni) compounds as published earlier,[6] indicating its impurity or defect like nature and its inhomogeneous distribution among the sample batch. Clearly species $U_2$ cannot be attributed to $Cu^{2+}$-$Cu^{2+}$ paddlewheel units in the **op** phase, since their signal is known from measurements on DUT-8(Cu) (Figure S8). We can only speculate, if species $U_2$ is some minor fraction of $Cu^{2+}$-$Cu^{2+}$ paddlewheels in the **cp** phase. The signal of species $U_2$ was also observed at $T$ = 14 K but its EPR intensity increases slightly with increasing temperature (Figure 3c), indicating an antiferromagnetic coupling with correspondingly small J-coupling, in case species $U_2$ is a dinuclear species. Unfortunately, our attempts to simulate the EPR signal of species $U_2$ more accurately than shown in Figure S11, failed. This failure might be attributed to correlated g- and zfs-strain effects which are not covered by the restricted linewidth model implemented in the MatLab toolbox EasySpin used for the spectral simulations.[1]

For sample $\mathbf{2}_{\mathbf{sol}}$ at $T$ = 14 K (Figure 4a and Figure 6a and b) a small signal (*) at $g \approx 2.06$ might be assigned to some minor monomeric $Cu^{2+}$, $Ni^{+}$ or $Ni^{3+}$ species. The signal ~ in Figure 4a might be attributed to some monomeric $Co^{2+}$ ($S$ = 1/2)[2] or some low spin $Co^{2+}$-$Ni^{2+}$ ($S$ = 1/2) species with g-tensor principle values $g_x = 2.620 \pm 0.008$, $g_y = 2.580 \pm 0.008$ and $g_z = 1.805 \pm 0.008$ as well as hfi-tensor principle values $|A_x| = 460 \pm 25$ MHz, $|A_y| = 435 \pm 25$ MHz and $|A_z| = 445 \pm 20$ MHz.

The low temperature EPR spectra of sample $\mathbf{2}_{\mathbf{act}}$ show a signal at about $B$ = 300 mT (Figure 7), which can be attributed to a $S$ = 1/2 species $U_{2act}$ with g-tensor principle values $g_x = 2.05 \pm 0.02$, $g_y = 2.15 \pm 0.08$ and $g_z = 2.40 \pm 0.15$. It might be attributed to minor monomeric $Ni^{+}$, low spin $Ni^{3+}$ or $Cu^{2+}$ species. No $^{63,65}Cu$ hfi was resolved but might possibly contribute to the linewidth of the signal.

Minor EPR signals measured for sample $\mathbf{2}_{\mathbf{res}}$ at $T$ = 14 K are illustrated in Figure 6c and d. Signal ~ and * are identically to the corresponding signals of sample $\mathbf{2}_{\mathbf{sol}}$ within the spectral resolution. Signal # is attributed to the same species as signal # in Figure 5a was attributed. The signal + at low fields might be again species $U_2$. One can speculate if its broad linewidth originates from magnetic interactions with neighboured magnetic centres, indicating that in sample $\mathbf{2}_{\mathbf{res}}$ species $U_2$ occurs in higher local concentrations than in sample $\mathbf{2}_{\mathbf{sol}}$. This broad linewidth might alternatively originate from zfs-strain effects due to a larger structural disorder in sample $\mathbf{2}_{\mathbf{act}}$ than in sample $\mathbf{2}_{\mathbf{sol}}$, induced by the adsorption of a larger amount of DMF in the former case.

## References

(1) Stoll, S.; Schweiger, A. EasySpin, a comprehensive software package for spectral simulation and analysis in EPR. *J. Magn. Reson.* **2006**, *178*, 42–55.

(2) van Doorslaer, S.; Jeschke, G.; Epel, B.; Goldfarb, D.; Eichel, R.-A.; Kräutler, B.; Schweiger, A. Axial solvent coordination in "base-fff" cob(II)alamin and related co(II)-corrinates revealed by 2D-EPR. *J. Am. Chem. Soc.* **2003**, *125*, 5915–5927.

(3) Hathaway, B. J.; Billing, D. E. The electronic properties and stereochemistry of mono-nuclear complexes of the copper(II) ion. *Coord. Chem. Rev.* **1970**, *5*, 143–207.

(4) TOMINAGA, H. Spectroscopic study of Cu(II) ions supported on silica gel by cation exchange method. *J. Catal.* **1975**, *40*, 197–202.

(5) Bon, V.; Klein, N.; Senkovska, I.; Heerwig, A.; Getzschmann, J.; Wallacher, D.; Zizak, I.; Brzhezinskaya, M.; Mueller, U.; Kaskel, S. Exceptional adsorption-induced cluster and network deformation in the flexible metal-organic framework DUT-8(Ni) observed by in situ X-ray diffraction and EXAFS. *Phys. Chem. Chem. Phys.* **2015**, *17*, 17471–17479.

(6) Mendt, M.; Gutt, F.; Kavoosi, N.; Bon, V.; Senkovska, I.; Kaskel, S.; Pöppl, A. EPR Insights into Switchable and Rigid Derivatives of the Metal–Organic Framework DUT-8(Ni) by NO Adsorption. *J. Phys. Chem. C* **2016**, *120*, 14246–14259.